



**HAL**  
open science

# Nematic liquid crystals light valve calibration and application to phase shifting speckle interferometry

Pierre Slangen, Benoit Gautier

## ► To cite this version:

Pierre Slangen, Benoit Gautier. Nematic liquid crystals light valve calibration and application to phase shifting speckle interferometry. Speckle06: Speckles, From Grains to Flowers, Sep 2006, Nimes, France. <10.1117/12.695272>. <hal-02012257>

**HAL Id: hal-02012257**

**<https://hal.science/hal-02012257v1>**

Submitted on 3 Jun 2021

HAL is a multi-disciplinary open access archive for the deposit and dissemination of scientific research documents, whether they are published or not. The documents may come from teaching and research institutions in France or abroad, or from public or private research centers.

L'archive ouverte pluridisciplinaire HAL, est destinée au dépôt et à la diffusion de documents scientifiques de niveau recherche, publiés ou non, émanant des établissements d'enseignement et de recherche français ou étrangers, des laboratoires publics ou privés.



HAL Authorization

# Nematic Liquid Crystals Light Valve Calibration and Application to Phase shifting Speckle Interferometry

Pierre Slangen, Benoit Gautier

CMGD MMS, Ecole des Mines d'Alès, 6 Av. de Clavières F-30319 ALES CEDEX France

## ABSTRACT

Liquid nematic crystals are nowadays more often used to change the polarization and/or phase and amplitude of impinging light wave. Nematic liquid crystals valves (LCLV) are also called SLM (Spatial Light Modulator) or LCVR (Liquid Crystal Variable Retarder). This paper will show the different steps required to get a procedure (optical mounting and computing software) enabling the use of LCLV in the output beam of the laser coupled with a 3D speckle interferometry set-up. This LCLV generates the phase shifts between the reference and object beams. The calibration set-up is made of a Mach Zender interferometer with the LCLV in one arm. Interference fringes are obtained and recorded with a CCD camera as LCLV voltage is increased. The fringe processing is achieved with a slice analysis in the Fourier domain. Required phase shifts are then implemented in the phase shifting software. The existing set-up already uses a phase shifter composed by a moving mirror driven by a piezoelectric transducer (PZT). Results of the calibration are compared between piezoelectric device and LCVR. The phase shifting rate and resulting phase error shows the main advantages of the LCVR. The whole set-up, with LCVR replacing the PZT, is finally applied to the determination of 3D displacement fields of Compact Tension Notch sample.

**Keywords :** LCLV, liquid crystals, calibration, speckle, interferometry

## 1. INTRODUCTION

Liquid Crystals Light Valves have been studied to modulate pure phase, pure amplitude or coupled “amplitude and phase” modulation [1]. LCLVs exist in single cell or in matrix configuration. This paper deals with single cell system. The existing set-up is working with a non-compensated piezoelectric crystal as phase retarder in the reference arm [2,3]. The expected assets of such LCLV system are a good linearity and a faster phase shifting rate. Moreover the LCVR is already mounted on a holder insuring an accurate mounting and avoiding the use of mechanical support of the PZT and also to cement the mirror on the PZT. While ordering the LCVR, it is important to specify the wavelength range and the phase shift amplitude. Some SLMs can not afford shifts lower than  $2\pi$  nor null phase shift if not compensated. To perform the LCVR calibration a Mach-Zender interferometer has been designed. The interferometric recombination of the two polarized impinging beams has been achieved using an analyzer at the exit of the interferometer. A polarizer can also be used in one arm, regarding the orientation of the valve versus the polarization of the laser. The interferometric fringes are then recorded with a CCD camera. The phase shift is generated by applying a voltage on the LCVR and is then computed by an appropriate algorithm. All the components including the laser head are driven by LabView softwares, including the post-processing (unwrapping, phase to displacement, display ...)

## 2. PHASE SHIFTING

### 2.1 Phase shift generation

Among the different systems generating phase shifts, the main families can be considered as shown on Figure 1. There is many others, but the most important one can never neglect, that is: the natural environmental drift of the interferometer. This drift can be generated by electronic noise, temperature or refractive index changes, mechanical vibrations, ...

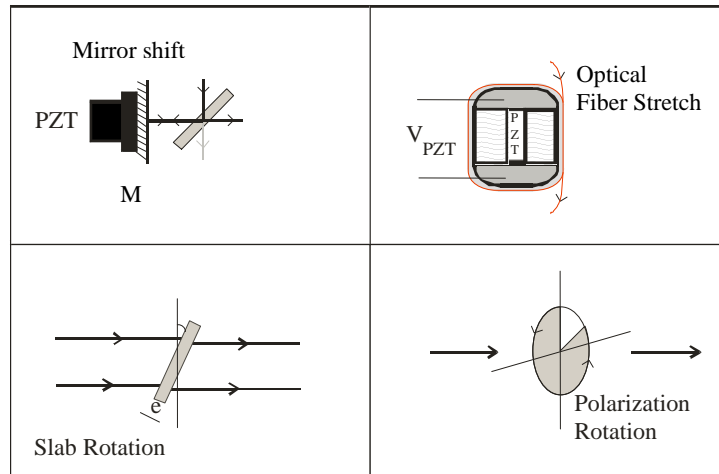


Fig. 1. Phase shifting generation

## 2.2 Piezoelectric transducer

Piezoelectrics transducers allow the translation of a mirror cemented at the top or to bend an optical fiber wrapped around. Two categories can be obtained: simple and compensated systems. The simple systems are cheaper but the hysteresis effect is not compensated whereas the compensated systems are limiting the hysteresis effect by acting on a retrofeedback loop (Fig.2). A recent study has also shown some random behaviors of the PZT [4].

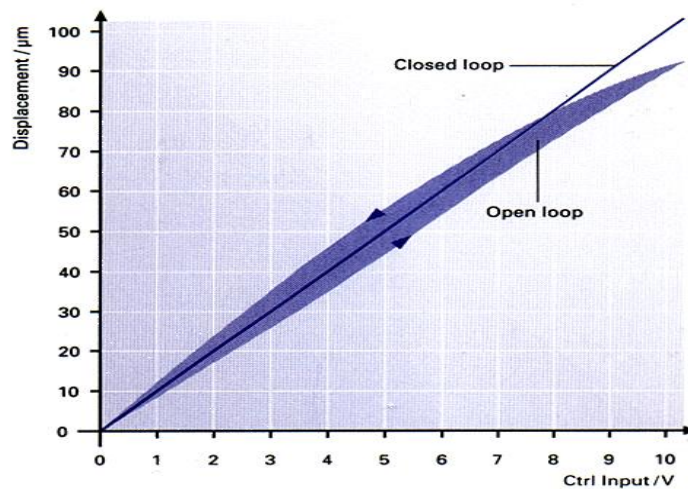


Fig. 2. Characteristic curve for PZT (from [www.physikinstrumente.com](http://www.physikinstrumente.com))

The ideal system might have the following characteristics

- Good linearity, long-term stability, repeatability and resolution
- Automatic compensation for different forces and loads
- Infinite rigidity (within the loads range)
- Hysteresis and creeps-effect rejection

The existing system uses a non compensated PZT rod with a cemented mirror moving along the incident laser beam. Two different problems occur: the hysteresis effect (Fig.3) and the requirement of many voltage orders sent to the system (time intervals of about 200ms).

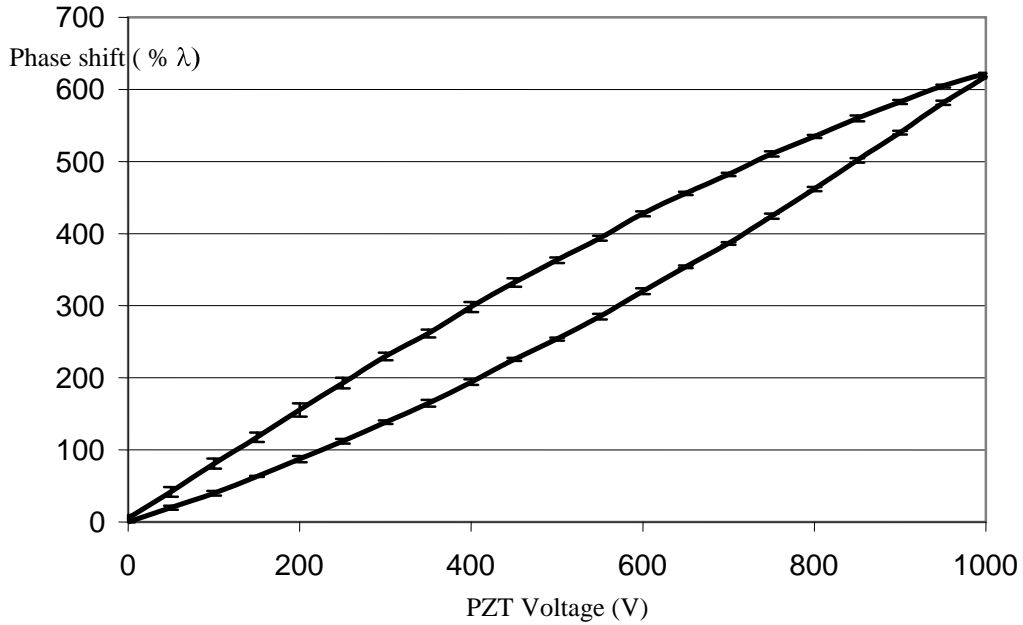


Fig. 3. Phase Shift versus Voltage for PZT non compensated

### 2.3 Liquid Crystals Variable Retarder

The LCVR architecture is showed in Figure 4. The system comes from Meadowlark<sup>®</sup> Optics, [model D3040](#). The faces of the cavity containing the birefringent material (liquid crystals) are made of three layers: Fused Silica Glass, Indium Tin Oxide (ITO, transparent conductor), and a polished dielectric layer insuring the molecules alignment thanks to microscopic parallel scratches. The two faces are separated with a spacer a few micrometers thick.

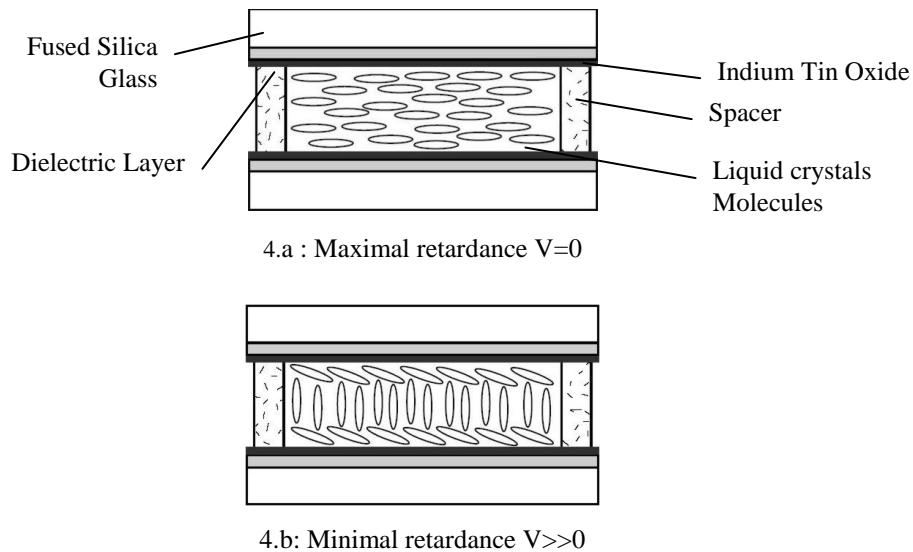


Fig. 4. LCVR Molecules alignment for  $V=0$  (a) and  $V>0$  (b)

The liquid crystals trapped in the layer cavity produce a single axis birefringent slab. The main characteristic of nematic materials is their main axis aligned together with their long axis parallel and a random distribution of their centers as shown in Figure 4. If no potential difference is applied between the ITO layers (Fig. 4a), the molecules hold aligned and parallel. The refractive index of extraordinary wave  $n_e$  is greater than the refractive index of ordinary wave  $n_o$ .

Equation 1 shows the maximal phase difference between ordinary and extraordinary beams, where  $\lambda$  is the wavelength of the light source and  $e$  the thickness of the single axis slab.

$$\phi = \phi_o - \phi_e = \frac{2\pi}{\lambda} (n_o - n_e) e \quad (1)$$

When the potential difference is applied between the ITO layers (Fig. 4b), molecules alignment comes to turn perpendicular to the silica glass plates. Hence the reduction of the refractive index difference occurs, and yielding to the phase difference decrease between the two beams.

We can mention the LCVR response time is related to the sign of the difference between final and initial voltage. This is linked to the molecules polarization direction (alignment voltage along or again the non-zero dipolar moment of the liquid crystals distribution).

### 3. CALIBRATION

The D3040 is used to generate phase shifts in our speckle interferometry set-up. The phase computing algorithm is “4 buckets”. The four shifted phase  $\phi_i$  ( $i=[0, 1, 2, 3]$ ), between reference and object beams are then:

$$\phi_0 = \phi, \phi_1 = \phi + \frac{\pi}{2}, \phi_2 = \phi + \pi, \phi_3 = \phi + \frac{3\pi}{2} \quad (2)$$

This algorithm is sensitive to phase shift miscalibration. A 10% error generates about  $\lambda/40$  uncertainty on the phase value [5]. 4-buckets is good balance between phase computing and acquisition time. The calibration of the LCVR has to be achieved before processing interferometric measurements.

The calibration “phase shift vs. voltage” curve (Fig. 5) is obtained for positive variations of 0.2V between successive recordings. The range to realize the 4 phase shifts is the linear zone between 1.7V and 2.4V. Refined measurements have qualified this linear aspect of the phase shift versus voltage. The final voltages obtained to get the required phase shifts are (1.7V, 1.918V, 2.136V, 2.354V). Each voltage ensures the expected shift within 10% accuracy. Moreover, we have noted the voltage rise step is linked to the response time of the valve. It is about 30ms for 0.2V step.

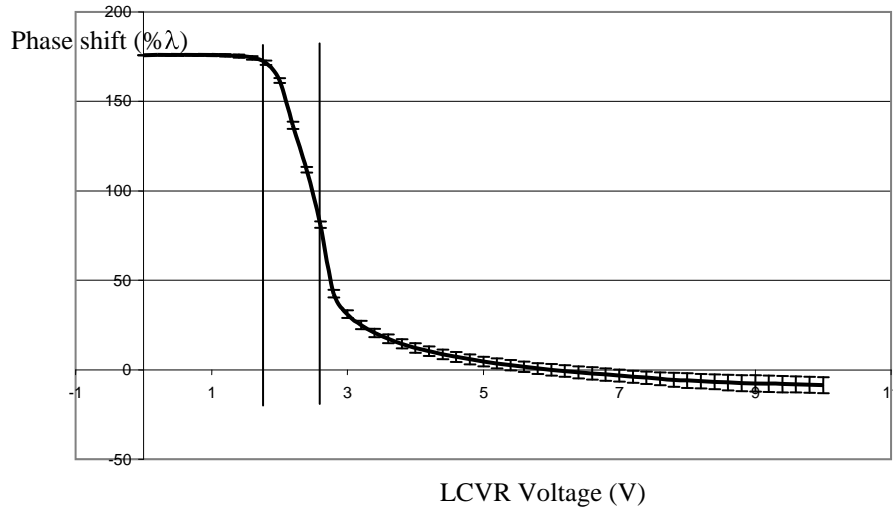


Fig.5. LCVR characteristic curve

### 4. ESPI MEASUREMENT

The LCVR has been placed in the reference arm of the Electronic Speckle Pattern Interferometry (ESPI) set-up. The slow axis is parallel to the laser polarization. The PZT has been kept in place to enable the results comparison with both

systems. The set-up is pure out of plane sensitive and the reference beam is uniform. The object beam impinges the plane surface of the calibration object. Phase shifted specklegrams, resulting of interference between object and reference beams, are collected for both phase shifting systems (PZT and LCVR) with the same camera and laser settings. Acquisition frame rate is 7im/s for about 1 megapixel image coded in 8 bits. The acquisition time for 4 phase shifted images is reduced from 1.3s for the PZT to 0.6s for the LCVR.

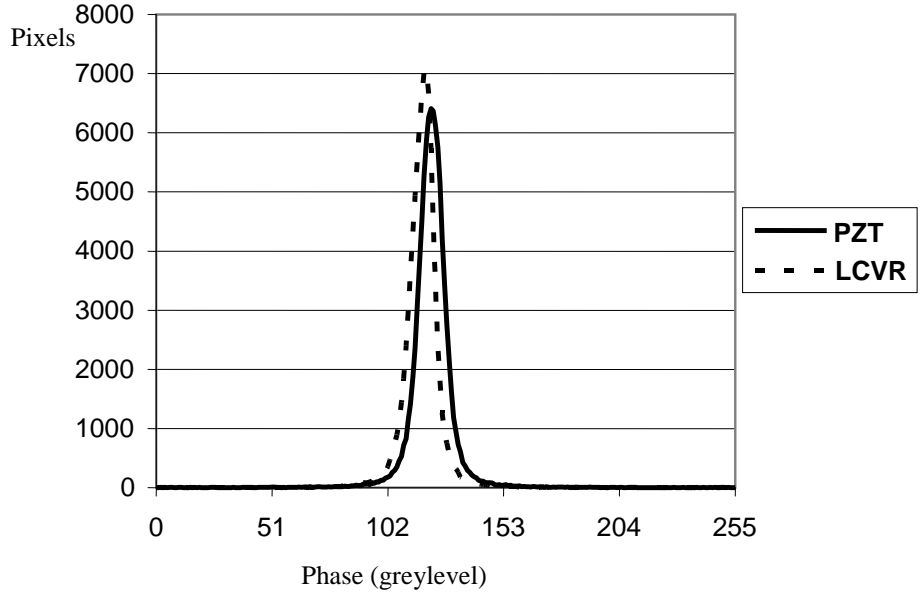


Fig.6. Histograms of the phase difference between two resting states (zero displacement)

The object is at rest. The histograms (Fig. 6) show the number of pixels with the same phase difference value is greater for the LCVR phase shift. The half-width value (around “zero-displacement” greylevel) is 9 greylevels for the LCVR and 10 greylevels for the PZT. The phase difference measurement uncertainty is then  $\lambda/25$  and  $\lambda/28$ , respectively. The slight difference between the results comes from the whole contribution of the acquisition set-up, that is the CCD non linearity, the phase shift error, and also the environmental stability. We point out that the gain of time coming from the LCVR switch enables to shorten the acquisition time so as to reduce the contribution of the environmental perturbations and then to decrease the measurement uncertainty.

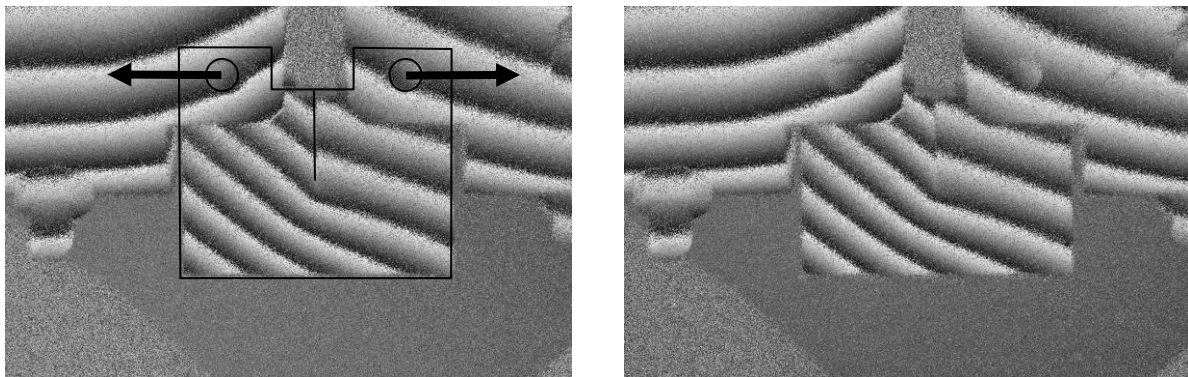


Fig.7. Wrapped phase difference between two loaded states for Compact Tension Notch Sample (PZT, left; LCVR right)

Fig. 7 presents the results for PZT (left) and LCVR (right) as phase shifter in our ESPI system applied to Compact Tension Notch Sample (sample drawn in black wire). The wrapped (and unwrapped) phase maps are really similar.

Experiments have also been performed with the LCVR in a 3D sensitive ESPI system, whether the displacement direction. These results enable the comparison between experiments and with numerical data from Finite Elements Modeling (Fig.8, 9) and show discrepancies of modeling near the notch.

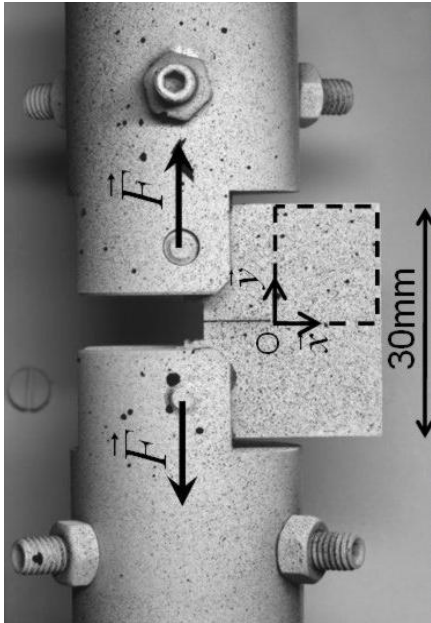


Fig.8. CTN Sample in test machine testing

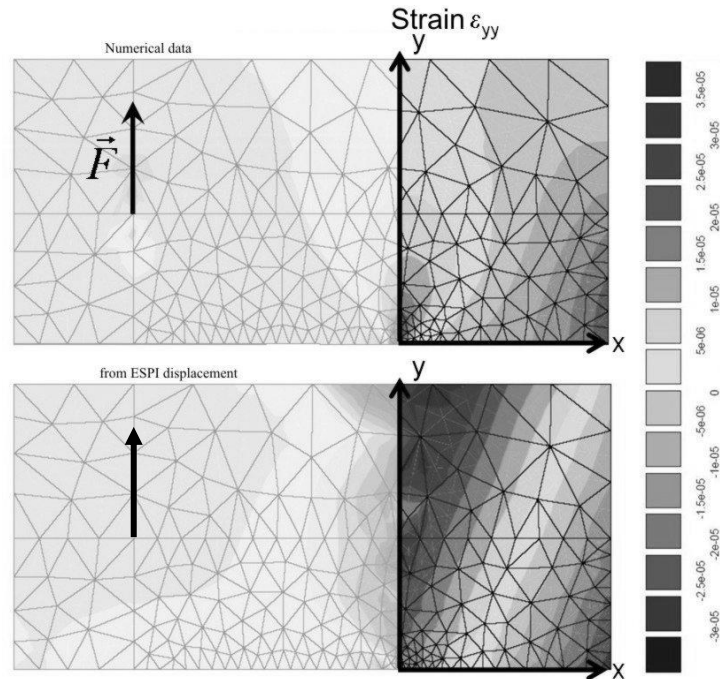


Fig.9. Numerical and ESPI derived  $\epsilon_{yy}$  strain maps

## 5. CONCLUSION

The replacement of piezoelectric transducer by a Liquid Crystals Light Valve enables to reduce the acquisition time of the specklegrams required to compute the phase state of an object in phase shifting ESPI. The uncertainty of the measurement is even slightly better for the LCVR phase shifter. Reducing acquisition time ensures faster process recording, and also to minimize the effects of environmental noise.

## REFERENCES

1. A. Jaulin, E. Hueber, L. Bigue, "Caractérisation de modulateurs spatiaux de lumière", Actes cinquième colloque francophone Méthodes et Techniques Optiques pour l'Industrie, CMOI SFO, Vol. 2, 319-324, Saint Etienne, France, 2004
2. [2] P. Slangen, C. De Veuster, Y. Renotte, L. Berwart, Y. Lion, "Computer-aided interferometric measurements of drift and phase shifter calibration for DSPI (Digital Speckle Pattern Interferometry)", *Opt.Eng.*, 34(12), 3526-3530, (1995)
3. [3] C. De Veuster, P. Slangen, Y. Renotte, L. Berwart, Y. Lion, "In-line phase-shifter calibration and drift measurement and compensation for digital speckle pattern interferometry (DSPI)", *Proc. SPIE-EOS*, Vol.2951, 117-124, (1996)
4. [4] D.N. Borza, "Champs de déplacements 3D à la surface d'un actionneur piézo-électrique et conséquences possibles pour l'utilisateur", Actes quatrième colloque francophone Méthodes et Techniques Optiques pour l'Industrie, CMOI SFO, Vol. 1, 205-210, Belfort, France, 2003
5. [5] R. Jones, C. Wykes, *Holographic and speckle interferometry*, Cambridge University Press Second Edition, 1989
6. [6] B. Gautier, P. Slangen, "Interféromètre de speckle à 3 directions d'éclairage: Calibration et applications", Actes quatrième colloque francophone Méthodes et Techniques Optiques pour l'Industrie, CMOI SFO, Vol. 1., 236-243, Belfort, France, 2003.